Optics Communications 382 (2017) 225–231

Contents lists available at ScienceDirect

Optics Communications

journal homepage: www.elsevier.com/locate/optcom

# Simple pre-distortion schemes for improving the power efficiency of SOA-based IR-UWB over fiber systems

H. Taki [a,b], S. Azou [b,*], A. Hamie [a,c], A. Al Housseini [a], A. Alaeddine [a], A. Sharaiha [b]

[a] Lebanese University, Faculty of Science I, LPE Research Center, Beirut, Lebanon
[b] ENIB/CNRS UMR 6285 Lab-STICC, Brest, France
[c] CRITC Research Center, Arts Sciences and Technology University in Lebanon (AUL), Lebanon

ARTICLE INFO

*Article history:*
Received 24 June 2016
Received in revised form
20 July 2016
Accepted 23 July 2016
Available online 7 August 2016

*Keywords:*
Ultrawideband (UWB) communications
Impulse radio (IR)
Semiconductor optical amplifier (SOA)
Nonlinear effects
Electrical pre-distortion
Power efficiency

ABSTRACT

In this paper, we investigate the usage of SOA for reach extension of an impulse radio over fiber system. Operating in the saturated regime translates into strong nonlinearities and spectral distortions, which drops the power efficiency of the propagated pulses. After studying the SOA response versus operating conditions, we have enhanced the system performance by applying simple analog pre-distortion schemes for various derivatives of the Gaussian pulse and their combination. A novel pulse shape has also been designed by linearly combining three basic Gaussian pulses, offering a very good spectral efficiency ( > 55%) for a high power (0 dBm) at the amplifier input. Furthermore, the potential of our technique has been examined considering a 1.5 Gbps-OOK and 0.75 Gbps-PPM modulation schemes. Pre-distortion proved an advantage for a large extension of optical link (150 km), with an inline amplification via SOA at 40 km.



## 1. Introduction

UWB is known to be a promising technology for short-range broadband wireless communications, thanks to its many interesting features including high data rate, immunity to multipath propagation, flexibility in reconfiguring data rate and power, very good time domain resolution, accurate mobile user location, and easy data protection [1,2]. Hence, UWB is a good candidate for various applications like local and wide area networks, sensor networks, emergency communications, radar, remote sensing, and military applications [3]. In 2002, the Federal Communication Commission (FCC) endorsed UWB devices to use the unlicensed frequency band [3.1,10.6] GHz, where the maximum emitted power must not exceed −41.3 dBm/MHz, in order to avoid interference with existing communication systems [4]. Impulse radio (IR), consisting in transmitting ultra-short duration pulses in baseband, is an attractive UWB technology due to its low cost and complexity [5,6]. Extending the coverage areas of UWB systems using optical fiber technology is a pertinent approach that has been demonstrated in recent studies [7–11]. UWB transmission over fiber requires direct optical pulse generation [12,13] or electro-optical conversion via intensity modulators [14]. In-line amplification is a key function for achieving the reach extension of any optical communication network. As low cost devices, semiconductor optical amplifiers (SOAs) [15] may be good candidates in the context of IR over fiber transmissions, the essence of IR being the simplicity with the objective of a wide use. Unfortunately, a main drawback for this approach is the non-linear effects inherent in the amplification, causing strong distortions in the propagating signals and a degradation in the power efficiency. Due to the regulation constraints associated to UWB free space propagation, highly efficient transmission is required which means that the pulse shapes must be preserved along the transmission in order to collect the maximum possible power under the FCC spectral mask. Hence, overcoming SOA non-linear distortions becomes a key objective. In the literature, numerous linearization techniques dealing with over fiber transmission have been investigated [16–18]. Here, we examine the potential of analog pre-distortion against SOA non-linearity by tuning some key parameters of pulses belonging to the Gaussian family or of their combinations [19], we have succeeded in designing highly efficient pulse shapes at the receiver side (photo-detector output). The best parameters of pre-distorted input pulses were extracted via global optimization based on the interior point algorithm. The resultant waveforms have been examined considering modulated IR signals; it is shown that a significant enhancement in the efficiency can be achieved for a large optical link extension, while operating at limited cost and complexity.

* Corresponding author.
*E-mail address:* azou@enib.fr (S. Azou).

http://dx.doi.org/10.1016/j.optcom.2016.07.066
0030-4018/

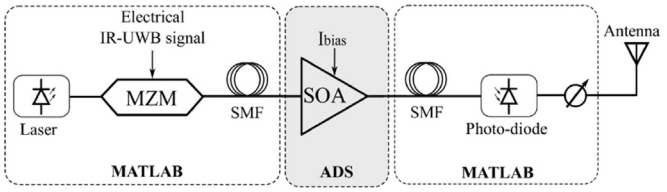


**Fig. 1.** Block diagram of the impulse radio over fiber system with Matlab/ADS co-simulation.

## 2. IR-UWB over fiber system architecture and SOA impact on output pulses response

The Radio-over-Fiber (RoF) utilized is depicted in Fig. 1. The transmitter relies on a Mach–Zehnder modulator (MZM) with half-wave voltage $V\pi$ of 6 V, biased at $V_{DC} = 1.5V_{\pi}$ by the electrical IR-UWB signal (with a peak-to-peak voltage $V_{pp}$), a continuous wave light being applied at its input (laser diode signal). The channel is made of a single mode fiber (SMF) and an in-line amplifier (SOA) for the reach extension purpose, with an injected bias current $I_{bias}$. At the receiver side (just before wireless transmission), a photo-detector converts the optical power into an electrical voltage signal to be eventually attenuated before entering the antenna (so as to meet FCC mask). The same ADS software-based model as in [20] is adopted for the SOA (INPHENIX-IPSAD1501), as it has proved to be highly accurate and in very good agreement with experimental data. Increasing the transmission distance requires operating in the saturated region of the SOA, which yields various nonlinear impairments affecting the transmitted signal. On the non-coherent receiver side, the resulting distortion will be characterized in terms of power efficiency with respect to the FCC mask, defined as:

$$\eta = \frac{\int_{3.1\ \mathrm{GHz}}^{10.6\ \mathrm{GHz}} S_p(f)\,df}{\int_{3.1\ \mathrm{GHz}}^{10.6\ \mathrm{GHz}} S_{FCC}\,df} \times 100\% \tag{1}$$

where $S_p(f)$ denotes the power spectral density (PSD) for a pulse $p(t)$ [19]. $\eta$ is computed after photo-detector while considering antenna effects are ignored. To have a look at SOA impact, Fig. 2 shows the spectral response of the 5th order derivative Gaussian pulse in electrical domain (solid-blue) and after being passed through SOA (dashed-green), without propagation in fiber. The PSD of the optical pulse violates FCC in the most restricted region corresponding to GPS band $[0.96–1.61]$ GHz, where the low power level ($-75.3$ dBm/MHz) is greatly challenging. So the average signal power has to be reduced so as to meet this limit, leading to a significant impact on the power efficiency (degradation > 30%). Hence, spectrum enhancement requires eliminating the low

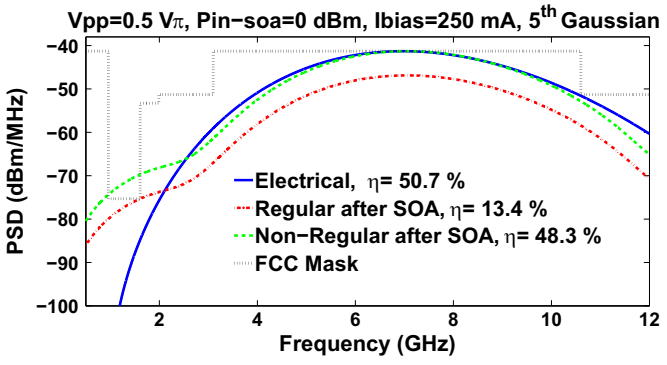


**Fig. 2.** Power spectral density of 5th Gaussian in electrical domain and after SOA (regular and irregular with FCC). (For interpretation of the references to color in this figure caption, the reader is referred to the web version of this paper.)

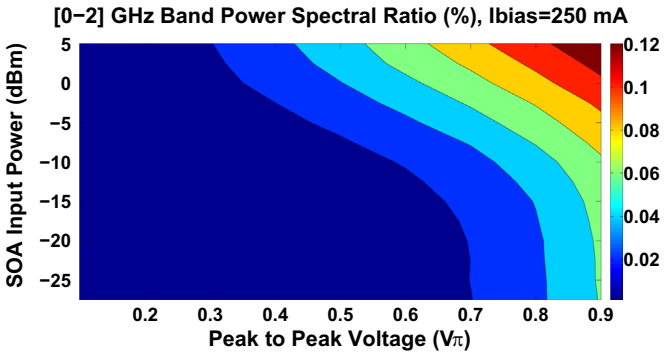


**Fig. 3.** $PSR_{2\ \mathrm{GHz}}$ of 5th Gaussian versus SOA input power and peak-to-peak voltage, where no fiber is considered.

frequency components induced by SOA. A simple criterion for evaluating this spectral impact corresponds to the ratio between the power collected in the [0,2] GHz band with respect to the overall PSD:

$$PSR_{2\ \mathrm{GHz}} = \frac{\int_0^{2\ \mathrm{GHz}} S_p(f)df}{\int_0^{\infty} S_p(f)df} \times 100\% \tag{2}$$

This criterion is analyzed in Fig. 3 for the case of the 5th derivative Gaussian pulse, with different peak-to-peak voltage and laser power, where $I_{bias} = 250$ mA. A quick rise of the PSR can be clearly observed, especially for $V_{pp} > 0.5V_{\pi}$ where strong nonlinearities act on the pulse waveform. In the following, we investigate the benefits of electrical pulse pre-compensation with the view to avoid any power efficiency degradation. The power efficiency of the 5th order Gaussian pulse is plotted in Fig. 4 versus SOA input power, for $I_{bias} = 250$ mA. When the amplified spontaneous emission (ASE) noise is ignored, a degradation in the power efficiency is observed as we move towards higher input powers. The bad impact of SOA particularly occurs at large $V_{pp}$ (e.g. $V_{pp} = 0.75V\pi$), where the drop in the efficiency results from the large spectral distortion. On the opposite, for $V_{pp} = 0.25V\pi$, a semi-linear gain behavior is ensured, leading to a very good spectral efficiency (approximately 50%) over a broad range of input power, reaching the saturation region (0 dBm). In the noisy case, the power efficiency is evaluated via Monte-Carlo simulations with the computation of the average over 100 runs; as can be clearly seen, the pseudo-linear gain characteristics is no longer preserved due to the larger noise influence at lower input power. Thus, there is a compromise between linearity and signal to noise ratio (SNR), which depends upon both the peak-to-peak voltage and the SOA input power. As can be seen, the ASE impact on pulse dynamics tends to be reduced for large $V_{pp}$; it is a positive aspect but at the

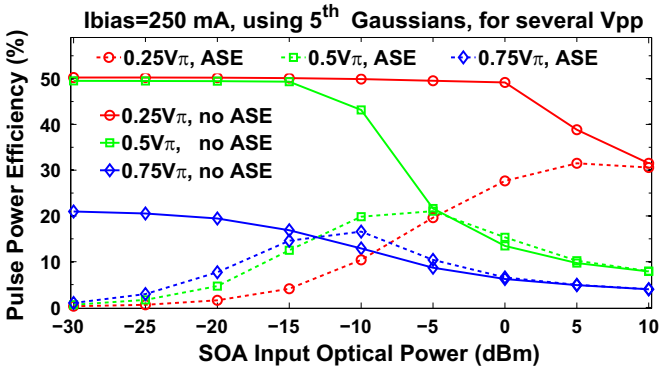


**Fig. 4.** Power efficiency of 5th Gaussian versus SOA input power for several peak-to-peak voltages, where no fiber is considered.

cost of nonlinearities. For $V_{pp} = 0.25V\pi$, the rise in efficiency is due to the increasing OSNR, combined with limited nonlinear effects. Prior to strong saturation, a slight increase in the efficiency ( < 5%) is noticed for the noisy signals over normal ones, for any $V_{pp}$, that is due to the power added by ASE noise within the UWB mask. We can systematically verify the convergence between solid and dashed lines at very high input power, resulting from a negligible noise power. For the remaining part of this paper, we will assume a medium value $V_{pp} = 0.5V\pi$, which is interesting in the sense that it both represents the noisy and nonlinear characteristics typically associated with SOA.

## 3. SOA nonlinearities mitigation via electrical pulses pre-distortion

A broad variety of linearization techniques is discussed in the literature [16–18,21] for reducing the nonlinear effects associated to optical communication systems. The different approaches can be classified into two main groups: electrical linearization and optical linearization. Optical schemes can operate over a wide bandwidth and some techniques are even specifically designed for SOA [22,23], but due to either high cost or bandwidth limitations associated to radio frequency control circuits, these schemes are not considered in our study. Regarding the methods operating in the electrical domain, digital linearization (pre-distortion are post-distortion) is interesting for its flexibility but we see the bandwidth/sampling requirements as a drawback for a low cost IR-UWB system; so, we preferred to investigate the alternative of analog pre-distortion, consisting in designing circuits at the transmitter side so as to suppress the nonlinear distortion components resulting from SOA amplification. As reported in various studies, tunable UWB pulse generators can be designed at low cost in CMOS technology [24–26]. Considering such techniques, we made the assumption of a tunable Gaussian pulse generator, so that the generated pulse $x(t, \mathbf{p})$ can be shaped with arbitrary parameters $\mathbf{p}$: shaping factor for the case of a single Gaussian pulse, or pulse shaping factors, weighting coefficients, besides the delay for a linear combination of Gaussian pulses. Then our aim is to identify the best tuning parameters $\mathbf{p}^*$ in the sense of a maximized power efficiency at the SOA output. In this study, we solve this global optimization problem via an interior point algorithm [27], using a numerical model of the component, as illustrated in Fig. 5. All distinct parameters are initialized at their optimum in electrical domain, so the algorithm can start from these values to re-optimize the pulse shape obtained at SOA output. Note that our approach presents some similarities with a work of Mirshafiei et al. [28], who addressed the pre-compensation against antenna effects, based on combinations of Gaussian pulses generated in the optical domain. Our contribution, whose a first investigation has been reported in [29], is different in the sense that we aim at mitigating SOA nonlinearities, which are very specific, and we consider that the pulses are generated/pre-distorted in the electrical domain. Regarding the practical aspect, this process could be automatically implemented in a closed loop transceiver system, utilizing software-to-hardware interfaces. In our setup, SOA was placed at 40 km, the operating point corresponding to an input power $P_{SOA} = 0$ dBm, which is a strong gain saturation point, while MZM is driven by $V_{pp} = 0.5V\pi$. These operating conditions are fixed for the remaining part of the study.

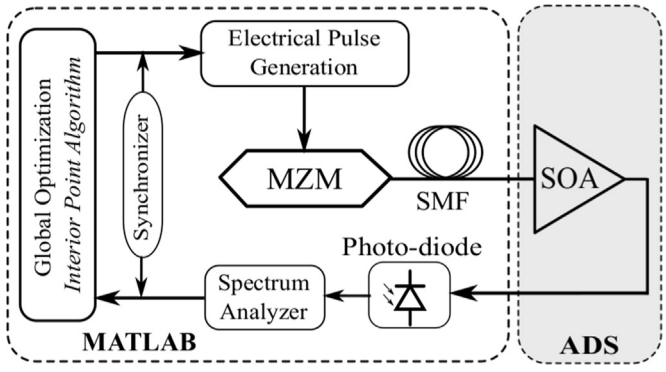


**Fig. 5.** Block diagram for the optimization process used for designing pre-distorted electrical waveforms.

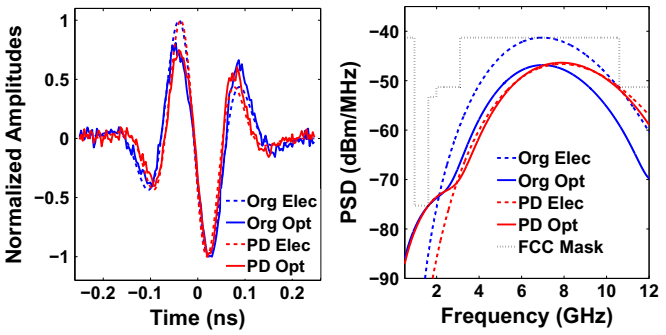


**Fig. 6.** Original (Org) and pre-distorted (PD) 5th Gaussian in electrical domain (Elec) and after SOA (Opt).

### 3.1. Case of 5th derivative Gaussian pulse

The high power efficiency offered by the 5th derivative Gaussian pulse, besides the acceptable order of generation complexity, both make it an attractive target for impulse radio system designers [30]. As shown in (3), only one variable could be calibrated in this waveform, which is the pulse shaping factor ($\sigma$). Such a parameter has a simultaneous influence on the 10 dB bandwidth ($B_{10}$) and on the central frequency. Fig. 6 describes the original and pre-distorted (PD) pulses in electrical domain and at SOA output, in the case of placing the photo-detector directly after SOA, where the spectra are plotted in the noise-free case (ASE noise not considered for spectrum readability). We can clearly see that the pre-distorted pulse exhibits only a small improvement in power efficiency ( < 5%), this is due to the single degree of freedom. Therefore it is better to search for more appropriate pulse shapes to be adopted with pre-distortion.

$$x_5(t) = \frac{A}{\sqrt{2\pi}}\left(\frac{-t^5}{\sigma^{11}} + \frac{10t^3}{\sigma^9} - \frac{15t}{\sigma^7}\right)\exp\left(-\frac{t^2}{2\sigma^2}\right) \tag{3}$$

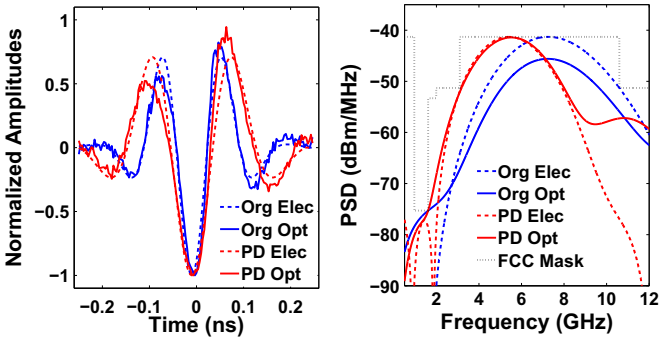


**Fig. 7.** Original (Org) and pre-distorted (PD) 6th Gaussian in electrical domain (Elec) and after SOA (Opt).

### 3.2. Higher order of Gaussian derivative

In reality, to avoid hitting the GPS band, the spectrum must be shifted towards higher frequencies. The spectral peak for any $n$th order Gaussian pulse derivative $x_n(t)$ is $f_{peak} = \frac{\sqrt{n}}{2\pi\sigma}$, where the spectrum is expressed as

$$X_n(f) = A(j2\pi f)^n \exp\left(-\frac{(2\pi f\sigma)^2}{2}\right) \tag{4}$$

To step up the power spectral density under FCC, we have to reduce $B_{10}$ by utilizing higher values of $\sigma$, as illustrated in (4). Increasing $\sigma$ can be compensated by augmenting $n$, hence making a separate control for $B_{10}$ and $f_{peak}$. Adopting a higher order of derivation gains more flexibility in shaping the spectrum, as the latter being far from the most severely power-restricted band (corresponding to GPS), and consequently the design of a pre-distorted waveform becomes much easier. The benefit of the 6th derivative Gaussian appears in Fig. 7, with a time domain expression given in (5). By lowering the 10 dB bandwidth of the pre-distorted pulse spectrum, we have enabled an increase in the efficiency ( > 20%) without violating the regular limit. In this case, the pre-distortion block could be implemented as a simple differentiator, which can enhance the performance at limited complexity.

$$x_6(t) = \frac{A}{\sqrt{2\pi}}\left(-\frac{15}{\sigma^7} + \frac{45t^2}{\sigma^9} - \frac{15t^4}{\sigma^{11}} + \frac{t^6}{\sigma^{13}}\right)\exp\left(-\frac{t^2}{2\sigma^2}\right) \tag{5}$$

### 3.3. Abraha's combination of Gaussian doublets

Good results have been achieved with single pulse pre-distortion; unfortunately, the number of adjustable parameters limits the improvement in the spectral efficiency. A more effective technique is to apply a combination of waveforms, in order to get a superior control of the resultant pulse dynamics, as will be presented in the sequel. Some combinations have been proposed in the literature [31,32], but taking into account practical constraints, it is better to conserve simple combinations within the Gaussian family. We have considered the work of Abraha et al., who have recently developed highly effective pulse shapes based on either monocycles or doublets [19]. As the latter approach relies on higher order of Gaussian derivative, with a better spectral efficiency, it will be the candidate in our work. Hence, two basic doublets $x_{21}(t)$, $x_{22}(t)$ will be considered, having different weighting coefficients and shaping factors:

$$C_D(t) = a_1 x_{21}(t) + a_2 x_{22}(t-\tau) \tag{6}$$

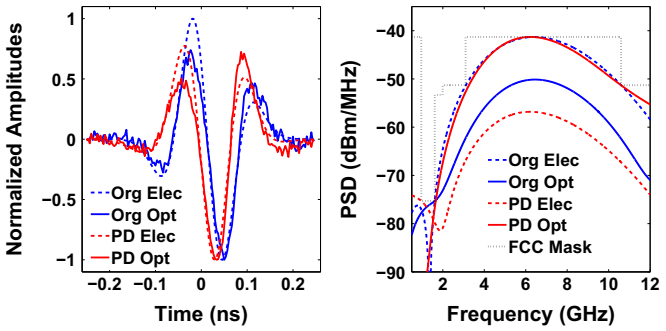


**Fig. 8.** Original (Org) and pre-distorted (PD) $C_{Doub}$ in electrical domain (Elec) and after SOA (Opt).

$$x_{2i}(t) = \frac{A}{\sqrt{2\pi}\sigma_i^3}\left(k\frac{t^2}{\sigma_i^2} - 1\right)\exp\left(-\frac{t^2}{2\sigma_i^2}\right) \tag{7}$$

$a_1$ and $a_2$ are the weighting factors, $\tau$ is a time delay between pulses, fixed at $\tau$=25 ps, and $k$=1.16 is an arbitrary scaling of the modified doublet. Table 1 displays all the parameters of utilized pulses, besides the power efficiencies in electrical domain and at SOA output (the spectral characteristics being evaluated at this point). $BL_{34}$ is defined as the left −34 dB bandwidth (frequency space between $f_L$ and $f_{peak}$), this criteria is useful to evaluate the spectrum in correspondence with GPS band. The term $A$ is always set at 1, as it has no influence on time dynamics for single waveforms; and in case of combinations, only the relative amplitude between basic pulses is important, since the real intensity for signals at photo-detector output is controlled by the laser power and peak-to-peak voltage. In Abraha's work, the doublets are similar with opposite polarities, as a high pass filtering is made via spectral oscillating term resulting from time delay. We do not preserve these conditions with pre-distortion, as the target is to mitigate SOA non-linearity by exploiting all the degrees of freedom associated to the linear combination of pulses. Hence, different shaping factors and weighting coefficients have been considered in our work. A significant jump in the power efficiency ( > 45%) is illustrated in Fig. 8 for the pre-distorted combination of doublets. The increase in the 10 dB bandwidth from 6.84 GHz to 7.34 GHz has enlarged the spectral coverage area under FCC mask, besides the 1.5 GHz reduction in $BL_{34}$, which permits a step up in the PSD without exceeding GPS limit. The peak of the spectrum exactly matches FCC limit (−41.3 dBm/MHz) at $f_{peak}$ = 6.2 GHz, which is not so far from the center of the UWB mask, thanks to pre-distortion.

### 3.4. A new waveform based on a combination of fundamental Gaussians

Increasing the number of tuning parameters in a waveform has shown to be more pertinent for pre-distortion. A new pulse shape

**Table 1**
Parameters ($\sigma_1$, $\sigma_2$, $\sigma_3$, $a_2/a_1$, $a_3/a_1$) of electrical generated pulses and the spectral characteristics ($f_{peak}$, $B_{10}$, and $BL_{34}$) of corresponding waveforms at SOA output (placed at 40 km). Besides the power efficiencies (%) in electrical domain and after SOA, with $P_{SOA}$ = 0 dBm, $I_{bias}$ = 250 mA, and $V_{pp} = 0.5V_\pi$.

| Pulses | $\sigma_1$ (ps) | $\sigma_2$ (ps) | $\sigma_3$ (ps) | $a_2/a_1$ | $a_3/a_1$ | $\eta$ (%) Elec | $f_{peak}$ (GHz) | $B_{10}$ (GHz) | $BL_{34}$ (GHz) | $\eta$ (%) SOA |
|---|---|---|---|---|---|---|---|---|---|---|
| Original 5th Gaussian | 51 | x | x | x | x | 50.7 | 7 | 6.17 | 6.11 | 13.7 |
| Pre-distorted 5th Gaussian | 45.07 | x | x | x | x | 15.74 | 7.86 | 6.95 | 6.88 | 17.2 |
| Original 6th Gaussian | 53.83 | x | x | x | x | 47.94 | 7.23 | 6.13 | 6.41 | 17 |
| Pre-distorted 6th Gaussian | 72.45 | x | x | x | x | 37.28 | 5.5 | 4.85 | 3.92 | 38 |
| Original $C_D$ | 43.02 | 43.02 | x | −1 | x | 57.2 | 6.45 | 6.84 | 6.05 | 6.96 |
| Pre-distorted $C_D$ | 61.68 | 40.47 | x | −1.24 | x | 1.6 | 6.2 | 7.34 | 4.56 | 54.1 |
| Original $C_G$ | 34.27 | 83.96 | 49.98 | 0.12 | −0.89 | 56.47 | 6.13 | 6.74 | 3.81 | 7.1 |
| Pre-distorted $C_G$ | 80.71 | 60.71 | 28.03 | 2.81 | −3.3 | 1.53 | 6.1 | 7.45 | 4.35 | 56.1 |

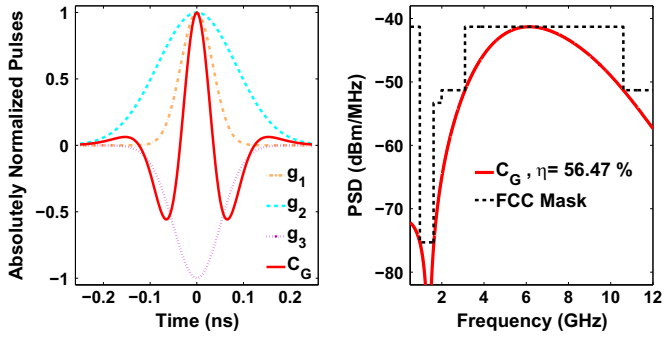


**Fig. 9.** Our proposed combination $C_G$ based on the pulses $g_i$ in time (left) and frequency (right) domain.

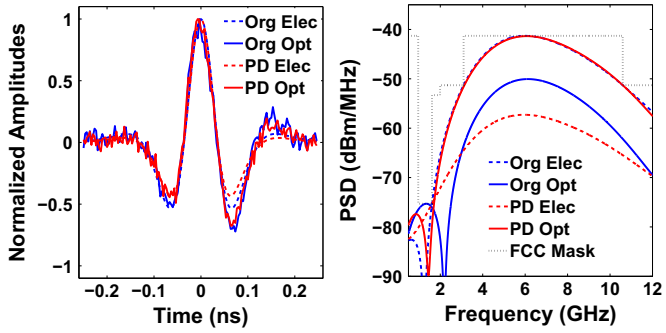


**Fig. 10.** Original (Org) and pre-distorted (PD) $C_G$ in electrical domain (Elec) and after SOA (Opt).

is now proposed, based on a linear combination of three fundamental Gaussian pulses:

$$C_G(t) = a_1 g_1(t) + a_2 g_2(t) + a_3 g_3(t) \tag{8}$$

where

$$g_i(t) = \exp\left(-\frac{t^2}{2\sigma_i^2}\right) \tag{9}$$

Such a combination enables a pre-distortion with 5 variables ($\sigma_1$, $\sigma_2$, $\sigma_3$, $a_2/a_1$, $a_3/a_1$), which promises for a better power efficiency obtained at SOA output. The weighting coefficients have been optimized as described in Table 1. The resultant waveform is depicted in Fig. 9 (left); it has a negligible DC component due to the opposite polarities of Gaussian amplitudes, with an energy being concentrated at a higher frequency range due to zero crossings. The peak frequency is 6.14 GHz, where the 3 dB and 10 dB bandwidths are $B_3$=4.1 GHz and $B_{10}$=7.5 GHz respectively, which is in very good agreement with the UWB spectral mask. As illustrated

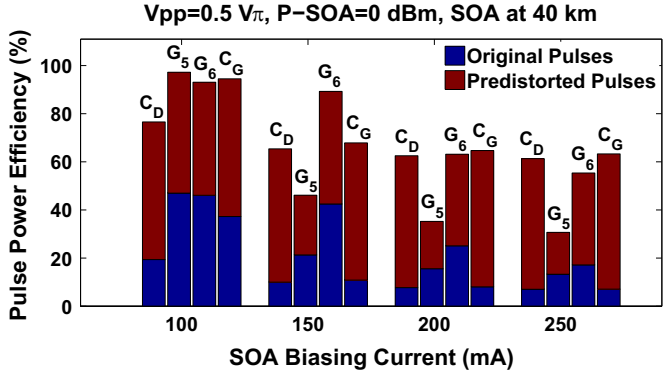


**Fig. 11.** Power efficiency of original and pre-distorted pulses directly after SOA (at 40 km) for several biasing currents.

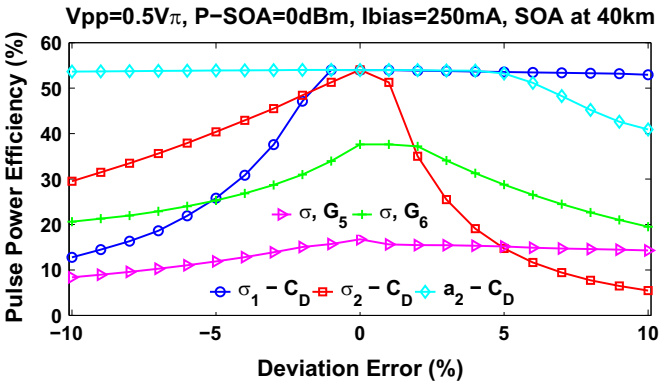


**Fig. 12.** Robustness against uncertainty for the 5th and 6th Gaussian pulses, besides Abraha's combination of doublets.

in Fig. 9 (right), a highly efficient pulse waveform is obtained, offering a power efficiency of $\eta$=56.47%, which outperforms the 5th derivative Gaussian pulse (50.7%) and is close to Abraha's combination of doublets (57.2%) in electrical domain. An important feature associated with our approach is the absence of any time differentiator nor delay line, which reduces the system cost and complexity [19,30,33]. As can be seen in Fig. 10, our combination has carried out the best power efficiency at SOA output ($\eta$=56.1%), which performs better than Abraha's combination of doublets (54.1%), thanks to the larger number of tuning parameters. After SOA, the pre-distorted spectrum has a close peak frequency to the original one (6.1 GHz), but covering a larger 10 dB bandwidth (7.45 GHz). Here there is a special case, the original spectrum at SOA output hits FCC mask at low frequencies due to the presence of a significant left side lobe, the main lobe staying far from the FCC limit even at the 34 dB band. This spectral characteristic results from the combining of time spread and windowing effect, which can be efficiently overcome by designing a pre-distorted pulse (better distribution of the pulse energy inside the time window). Because the pulse undergoes a time spread after amplification the energy outside the 0.5 ns slot is no more negligible, which translates into significant sidelobes in frequency domain (*sinc* influence). The pre-distortion processing has enabled a significant change in the pulse dynamics so as to render this time windowing effect negligible.

### 3.5. Bias current influence

Efficient pulses in electrical domain are usually more affected by the optical system non-linearity. We can see in Fig. 11 that for low biasing currents (100 mA), the 5th and 6th Gaussian pulses have a small degradation in the power efficiency; whereas a

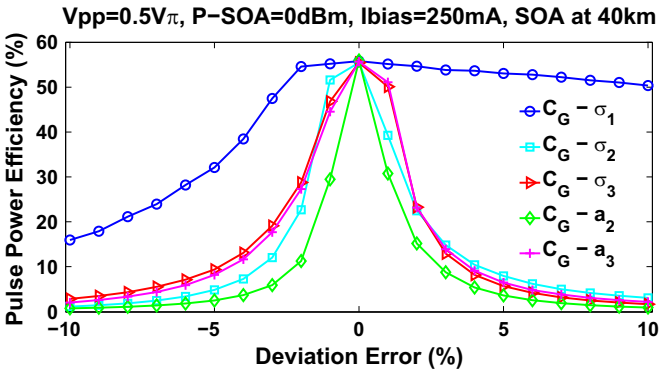


**Fig. 13.** Robustness against uncertainty for our proposed pulse based on fundamental Gaussians.

significant decrease ( > 30%) is noticed for the combination of doublets. Applying a larger biasing current increases the order of nonlinearity, which leads to lower spectral efficiencies for all pulses. Nevertheless, we observe that no great change occurs after 200 mA, due to the optical gain saturation at 0 dBm input power. Pre-distortion could be applied with all biasing currents, but with the view to achieve a reach extension the value of 250 mA is adopted, as associated with the highest optical power at SOA output. For such conditions, our pre-distorted pulse offers a neat advantage over the 5th or 6th derivative Gaussian waveforms and is slightly more effective than Abraha's pre-distorted pulse.

### 3.6. *Robustness against uncertainty for single waveforms and combinations*

Until now only theoretical models have been considered for the different pulse shapes. But from a practical point of view, some uncertainties are expected to occur in the CMOS circuits that could be designed to generate the various pulses. So, we investigate in this sub-section the impact of any parametric deviation with respect to the optimum solution discussed previously. Fig. 12 illustrates how the power efficiency is affected by a parametric uncertainty for the 5th and 6th Gaussian pulses, together with the doublets combination. $G_5$ and $G_6$ show a kind of immunity against systematical errors, as $\sigma$ is the unique variable which controls the dynamics of a single pulse. The problem appears with Abraha's combination, which exhibits a relative robustness against $\sigma_1$ and $a_2$ deviations; unfortunately, any slight change in $\sigma_2$ is enough to drop off the spectral efficiency, specially for negative deviation errors, knowing that it is not a simultaneous change in the combination variables. We can figure out that the newly designed pulse is the most sensitive against system uncertainties, as illustrated in Fig. 13. In fact, it is much more influenced than the other waveforms, as it relies on a larger number of pulses, and all parameters have been optimized simultaneously, so any change in one of the variables makes all the set no more optimal. Besides, pure Gaussian pulses have strong DC component, which can reappear in our combination due to any lose in the basic pulses symmetry (positive/negative symmetry which cancels the DC), and consequently lead to a fast drop in the power efficiency ($\eta < 5\%$ for a deviation error of 10%).

## 4. Case of a modulated impulse radio signal propagating over optical fiber link

In our simulations, we take into account the effects of the optical link (attenuation and chromatic dispersion) before SOA, as they have an influence on the pulse dynamics entering the amplifier, depending on the covered distance, fiber input power, and peak-to-peak power swing. Therefore, the optimum parameters of pre-distorted waveforms have been extracted considering SOA located at 40 km, where the operating conditions are the same as mentioned in Table 1. In order to evaluate our pre-distortion scheme considering a stream of modulated pulses, a new criterion of power efficiency has been defined as

$$\eta_M = \frac{P_{\mathcal{F}}}{\max(\overline{P_{\mathcal{F}}})} \tag{10}$$

where $P_{\mathcal{F}}$ stands for the power collected over a frequency band of interest $\mathcal{F}$ (typically the [3.1–10.6] GHz band) for the electrical signal at antenna input, and $\max(\overline{P_{\mathcal{F}}})$ denoting the total power evaluated over the same band for an OOK or PPM modulated signal based on the *sinc* pulse, which is optimal in the sense that it corresponds to a 100% spectrum use (full coverage of the spectral mask). The advantage of pre-distortion is depicted in Fig. 14 for a

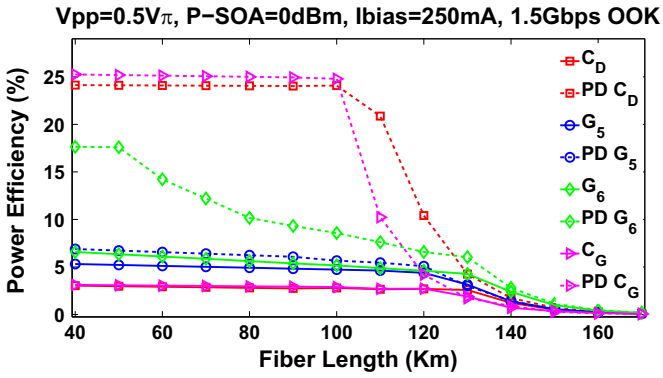


**Fig. 14.** Power efficiency versus fiber length for 1.5 Gbps OOK based on the utilized pulses, P-SOA=0 dBm, $I_{bias}$ = 250 mA, $V_{pp} = 0.5V\pi$, where SOA is placed at 40 km.

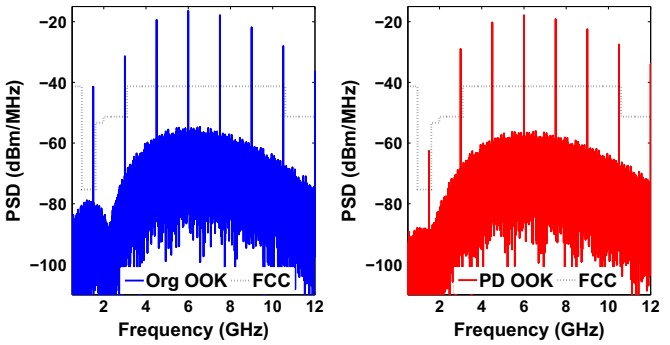


**Fig. 15.** Irregular PSD of 1.5 Gbps OOK based on original (left) and pre-distorted (right) $C_G(t)$ after SOA (at 40 km), where P-SOA=0 dBm, $I_{bias}$ = 250 mA, $V_{pp} = 0.5V\pi$.

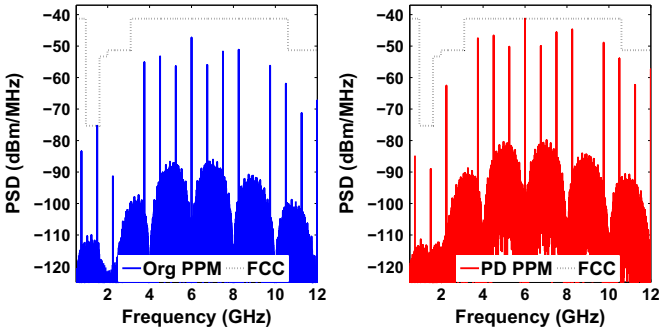


**Fig. 16.** Regular PSD of 0.75 Gbps PPM based on original (left) and pre-distorted (right) $C_G(t)$ after SOA (at 40 km), where P-SOA=0 dBm, $I_{bias}$ = 250 mA, $V_{pp} = 0.5V\pi$.

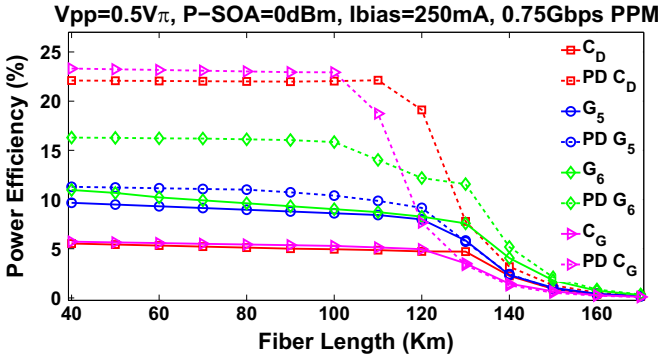


**Fig. 17.** Power efficiency versus fiber length for 0.75 Gbps PPM based on the utilized pulses, P-SOA=0 dBm, $I_{bias}$ = 250 mA, $V_{pp} = 0.5V\pi$, where SOA is placed at 40 km.

1.5 Gbps OOK, so we can gain an improvement over a large enough traveling distance (40–150 km), knowing that no pre-amplifier has been placed for modulated signals before the antenna. The degradation in the curves is due to frequency shaping and deviation caused in fiber [9] (with a chromatic dispersion of 17 ps/nm/km), so the central frequency and $B_{10}$ are no more preserved specially at large extension link. This improvement is justified by the fact that, the envelope of spectral spikes for OOK or PPM takes the shape of basic transmitted waveform, so perfect pulse shapes lead to an efficient spectrum associated with the modulated impulse radio signal. Between 40 km and 100 km, we can see a flat response in the curves corresponding to combinations of pulses, which results from the fact that all spectra are already above FCC limit, thus the signal has to be systematically attenuated so as to respect the mask. Our waveform exhibits a faster degradation than doublets at large distances, as it has less immunity against fiber effects. Regarding practical aspects, we can say that power efficiency enhancement comes at the price of a larger complexity; depending on application constraints, adopting higher order of derivation with a single pulse shape could be more suitable than applying a combination of pulses, and utilizing a combination of two pulses may be much simpler than using a set of three pulses. The PSD of the $C_G$-based OOK signal at SOA output is plotted in Fig. 15, with no attenuation. Apparently, the spectral shaping at low frequency band is the reason beyond efficiency enhancement, so a higher power level can be achieved by the spectra when adapted to FCC mask, as shown in Fig. 16 for a 0.75 Gbps PPM. Fig. 17 proves that the same conclusion could be drawn for PPM regardless the covered distance in the optical link, where PPM index is 0.5 ns. Therefore, the proposed pre-distortion technique has always validated a good potential, while reaching a coverage of 150 km, fitting the request of Fiber-to-the-Home (FTTH) networks reported in the literature [34]. The improvement in the power efficiency translates into a higher signal-to-noise ratio obtained at the antenna output, which promises with a better bit error rate performance in energy detection receivers.

## 5. Conclusion

A low cost SOA in-line amplifier has been considered in this study for the purpose of reach extension of IR-UWB over fiber systems. Based on a realistic SOA physical model, analog pre-distortion schemes have been investigated for coping with SOA nonlinearities and with the view to improve power efficiency. Two linear combinations of Gaussian pulses were utilized, the first is based on Abraha's combination of doublets and the second has been newly designed based on pure Gaussians. Both have proved to be highly effective for correcting SOA impact. Using higher orders of Gaussian derivatives is an alternative solution offering a lower potential but with less complexity. Over a large extension of the optical link, our pre-distortion approach has exhibited an enhancement in the power efficiency of 1.5 Gbps-OOK and 0.75 Gbps-PPM. Experiments will be conducted in our future work so as to validate the proposed schemes, while considering bit error rate analysis and including antenna effects.

## References


[1] M. Ghavami, L. Michael, R. Kohno, Ultra Wideband Signals and Systems in Communication Engineering, John Wiley & Sons, UK, 2007.
[2] G.R. Aiello, G.D. Rogerson, Ultra-wideband wireless systems, IEEE Microw. Mag. 4 (2) (2003) 36–47.
[3] I. Oppermann, M. Hämäläinen, J. Iinatti, UWB: Theory and Applications, John Wiley & Sons, UK, 2005.
[4] FCC Report and Order, In the Matter of Revision of Part 15 of the Commission's Rules Regarding Ultra-Wideband Transmission Systems, FCC 02-48, April 2002.
[5] M.Z. Win, R.A. Scholtz, Impulse radio: How it works, IEEE Commun. Lett. 2 (2) (1998) 36–38.
[6] J.R. Fernandes, D. Wentzloff, Recent advances in IR-UWB transceivers: an overview, in: Proceedings of 2010 IEEE International Symposium In Circuits and Systems (ISCAS), 2010, pp. 3284–3287.
[7] C. Lim, A. Nirmalathas, M. Bakaul, P. Gamage, K.L. Lee, Y. Yang, R. Waterhouse, Fiber-wireless networks and subsystem technologies, IEEE J. Lightwave Technol. 28 (4) (2010) 390–405.
[8] F. Zeng, J. Yao, An approach to ultrawideband pulse generation and distribution over optical fiber, IEEE Photon. Technol. Lett. 18 (7) (2006) 823–825.
[9] S. Pan, J. Yao, Performance evaluation of UWB signal transmission over optical fiber, IEEE J. Sel. Areas Commun. 28 (6) (2010) 889–900.
[10] M. Popov, The convergence of wired and wireless services delivery in access and home networks, in: Optical Society of America in Optical Fiber Communication Conference, 2010, p. OWQ6.
[11] N.J. Gomes, M. Morant, A. Alphones, B. Cabon, J.E. Mitchell, C. Lethien, S. Iezekiel, Radio-over-fiber transport for the support of wireless broadband services, J. Opt. Netw. 8 (2) (2009) 156–178.
[12] F. Zeng, Q. Wang, J. Yao, All-optical UWB impulse generation based on cross-phase modulation and frequency discrimination, Electron. Lett. 43 (2) (2007) 119–121.
[13] M. Bolea, J. Mora, B. Ortega, J. Capmany, Optical UWB pulse generator using an N tap microwave photonic filter and phase inversion adaptable to different pulse modulation formats, Opt. Express 17 (7) (2009) 5023–5032.
[14] Y. Yu, J. Dong, X. Li, X. Zhang, Ultra-wideband generation based on cascaded Mach–Zehnder modulators, IEEE Photon. Technol. Lett. 23 (23) (2011) 1754–1756.
[15] M.J. Connelly, Semiconductor Optical Amplifiers, Kluwer, Boston, MA, 2002.
[16] K. Roberts, L. Chuandong, L. Strawczynski, M. O'sullivan, I. Hardcastle, Electronic precompensation of optical nonlinearity, IEEE Photon. Technol. Lett. 18 (1–4) (2006) 403–405.
[17] E. Ip, J.M. Kahn, Compensation of dispersion and nonlinear impairments using digital back propagation, J. Lightwave Technol. 26 (20) (2008) 3416–3425.
[18] A.J. Lowery, Fiber nonlinearity pre-and post-compensation for long-haul optical links using OFDM, Opt. Express 15 (20) (2007) 12965–12970.
[19] S.T. Abraha, C. Okonkwo, P.A. Gamage, E. Tangdiongga, T. Koonen, Routing of power efficient IR-UWB wireless and wired services for in-building network applications, J. Lightwave Technol. 30 (11) (2012) 1651–1663.
[20] H. Khaleghi, P. Morel, A. Sharaiha, T. Rampone, Experimental validation of numerical simulations and performance analysis of a coherent optical-OFDM transmission system employing a semiconductor optical amplifier, J. Lightwave Technol. 31 (1) (2013) 161–170.
[21] X. Zhang, R. Zhu, D. Shen, T. Liu, Linearization technologies for broadband radio-over-fiber transmission systems, Photonics 1 (4) (2014) 455–472.
[22] C. Tai, S.-L. Tzeng, H.-C. Chang, W.I. Way, Reduction of non-linear distortion in mqw semiconductor optical amplifier using light injection and its application in multichannel m-qam signal transmission systems, IEEE Photon. Technol. Lett. 10 (April) (1998) 609–611.
[23] F. Tabatabai, H.S. Al-Raweshidy, Feed-forward linearization technique for reducing non-linearity in semiconductor optical amplifier, J. Lightwave Technol. 25 (September (9)) (2007) 2667–2674.
[24] J. Han, C. Nguyen, Ultra-wideband electronically tunable pulse generators, IEEE Microw. Wirel. Compon. Lett. 14 (3) (2004) 112–114.
[25] H. Kim, Y. Joo, S. Jung, A tunable CMOS UWB pulse generator, in: Proceedings of the IEEE International Conference on Ultra-Wideband, Waltham, MA, September 24–27, 2006, pp. 109–112.
[26] R. Thai-Singama, F. Du-Burck, M. Piette, Demonstration of a low-cost ultra-wideband transmitter in the 3.1–10.6-GHz band, IEEE Trans. Circuits Syst.: Express Briefs 59 (July (7)) (2012) 389–393.
[27] J.E. Mitchell, P.P. Pardalos, M.G.C. Resende, Interior point methods for combinatorial optimization, in: D.-Z. Du, P. Pardalos (Eds.), Handbook of Combinatorial Optimization, vol. 1, Kluwer Academic Publishers, the Netherlands, 1998, pp. 189–297.
[28] M. Mirshafiei, M. Abtahi, L.A. Rusch, Ultra-wideband pulse shaping: bypassing the inherent limitations of the Gaussian monocycle, IET Commun. 6 (9) (2012) 1068–1074.
[29] H. Taki, S. Azou, A. Hamie, A. Al Housseini, A. Alaeddine, A. Sharaiha, Pulse shape pre-distortion for improving the power efficiency of SOA-based IR-UWB over fiber systems, in: 23rd IEEE International Conference on Telecommunications (ICT 2016), Thessaloniki, Greece, 16–18 May 2016.
[30] H. Jin, L. Jiang, W. Hao, C. Sheng, H. Qijun, Z. Yueping, A CMOS fifth-derivative Gaussian pulse generator for UWB applications, J. Semicond. 35 (9) (2014) 095005.
[31] M. Wang, S. Yang, S. Wu, A GA-based UWB pulse waveform design method, Digit. Signal Process. 18 (1) (2008) 65–74.
[32] M. Matsuo, M. Kamada, H. Habuchi, Design of UWB pulses based on B-splines, in: IEEE International Symposium on Circuits and Systems (ISCAS), 2005, pp. 5425–5428.
[33] H. Sheng, P. Orlik, A.M. Haimovich, Jr. L.J. Cimini, J. Zhang, On the spectral and power requirements for ultra-wideband transmission, in: IEEE International Conference on Communications, 2003 (ICC'03), vol. 1, 2003, pp. 738–742.
[34] R. Llorente, T. Alves, M. Morant, M. Beltran, J. Perez, A. Cartaxo, J. Marti, Ultra-wideband radio signals distribution in FTTH networks, IEEE Photon. Technol. Lett. 20 (11) (2008) 945–947.